physica status solidi a
www.pss-a.com

Temperature-Induced Transformation of the Atomic Configuration of the BO_2* Defect in Boron-Doped Czochralski Si

Lyudmyla Khirunenko, Mykhailo Sosnin, Andrii Duvanskii, and Nikolay Abrosimov*

In this study, the new data concerning the electronic and vibrational properties of the B_sO_{2i}* defect in Czochralski-grown boron-doped silicon are reported. In silicon subjected to treatment at elevated temperatures, a new boron-related defect is detected. An additional intracenter electronic transition for boron associated with the revealed defect is observed. The defect is identified as B_sO_{2i} due to the linear dependence of its formation efficiency on the boron content and the quadratic dependence on the oxygen concentration. The revealed complex is formed synchronously with the annealing of the previously identified B_sO_{2i}* defect. The detected complex is formed as a result of temperature transformation of the atomic configuration of the B_sO_{2i}* defect. The transformation occurs with activation energy of 2.59 eV. The local vibrational modes associated with both configurations of the B_sO_{2i}* complex are identified. The results of the study suggest that the B_sO_{2i}* defect in both configurations exists in a wide temperature interval, impacts the optical and electronic properties of the material, and must be taken into consideration when developing Si:B-based devices.

1. Introduction

Until now, silicon remains to be a subject of active research because of its wide application in such areas as the conventional electronic industry, power electronics, fabrication of solar cells, and quantum technology. The development of modern devices based on silicon with given properties demands first of all the production of materials with required electrophysical parameters. The latter are determined, to a great extent, by impurities and lattice defects. On the one hand, defects create the key functional abilities of semiconductor devices by affecting the concentration, mobility, and lifetime of charge carriers or by participating in optical transitions. On the other hand, they can cause a substantial degradation of the device efficiency, for example, by enhancing undesirable recombination of current carriers.[1–3] In particular, understanding the interaction of boron with the main technological impurities is important for improving the parameters of solar photoconverters produced from Czochralski-grown boron-doped silicon because the main factor affecting the efficiency of solar cells is the bulk recombination of charge carriers at lattice defects.[3–7]

Boron doping is widely used in modern mono- and multisilicon-based microelectronics, as well as in creation of submicron Si devices. Therefore, studies of boron-related defects in Si are of great importance. The interaction of substitutional boron atoms with oxygen dimers has been an intensively studied topic for boron-doped Si in recent years. This interest emerged because of the light-induced degradation (LID) of solar cells fabricated on the basis of this material, which is observed during the first hours of their operation. The degradation was attributed to the formation of BO_2 centers with enhanced recombination activity.[3,6]

A large number of theoretical and experimental investigations were devoted to the study of the properties of B_sO_{2i} defects in Cz-Si, as well as the models of their structural configurations. The research results showed that boron atoms can interact with oxygen dimers in the course of the initial material production, at the injection of current carriers, due to illumination and elevated temperatures.[8–23]

Various models of stable structural configurations were proposed for B_sO_{2i} complexes. The models differ in the bonds between the substituting boron atom and the two oxygen atoms in the B_sO_{2i} structure. In some studies,[12,24,25] the existence of direct bonds between the boron atom and two oxygen atoms in the stable configuration of B_sO_{2i} complex is considered, whereas the other authors[14,23,26] assume that the oxygen atoms are the second nearest neighbors of the boron atom.

According to ab initio modeling of B_sO_{2i} complexes, it was found that, similarly to the dimers, they can exist in two stable configurations—square and staggered.[14,24–26] The oxygen is three coordinated in the square configuration and two coordinated in the staggered one. However, irrespective of the models proposed for B_sO_{2i} complexes, the authors suggest the possibility for the complex to transform between the configurations.

The modification of the atomic structure configuration can affects the electronic properties of Si:B-based devices.

L. Khirunenko, M. Sosnin, A. Duvanskii
Institute of Physics
National Academy of Sciences of Ukraine
Prospekt Nauky 46, 03028 Kyiv, Ukraine
E-mail: lukh@iop.kiev.ua

N. Abrosimov
Department of Classical Semiconductors
Leibniz-Institut für Kristallzüchtung
Max-Born Str. 2, 12489 Berlin, Germany

The ORCID identification number(s) for the author(s) of this article can be found under https://doi.org/10.1002/pssa.202400484.

DOI: 10.1002/pssa.202400484

For instance, the change in the atomic configuration of B_sO_{2i} is associated with a new mechanism of LID of solar cells recently proposed by Vaqueiro-Contreras et al.[23] When studying the diodes fabricated on the base of boron-doped Cz-Si by deep level transient spectroscopy, the authors detected a deep donor that was observed in as-fabricated diodes. Under the action of light or the injection of minority carriers, the revealed donor transforms into a recombination active shallow acceptor responsible for solar cells degradation. It is assumed that both the deep donor and shallow acceptor are B_sO_{2i} complexes and during the donor–acceptor transformation, the configuration of the B_sO_{2i} complexes changes from square to staggered. It should be noted that according to the defect models considered in the study, the boron atom does not form direct bonds with two oxygen atoms in both configurations.[23] The oxygen atoms are the second nearest neighbors of the boron atom.

Recently, while studying the absorption spectra of Cz-Si doped with boron, we have detected one more defect arising owing to the interaction between the boron atoms and the oxygen dimers. Unreported previously transitions in the spectral range corresponding to the intracenter electronic absorption for boron with maximum at 228 and 261.3 cm^{-1} were detected in samples subjected to treatment at elevated temperatures.[27,28] The revealed spectral lines were found to be shifted toward low frequencies with respect to the main ones for boron. The concentration of defects associated with the detected absorption lines depends linearly on the boron concentration and quadratically on the oxygen content in the Cz-Si samples. Therefore, the defect responsible for the appearance of these lines was identified as the B_sO_{2i}* complex.

The revealed defect does not result in the LID for solar cells. The defect anneals out at a temperature of about 550 °C, which is different from an annealing temperature of 200 °C for BO_2, which leads to the LID. Besides we did not observe any changes in the intensity of detected absorption lines for the samples subjected to exposure to the illumination with light close in a spectral composition to solar radiation with an intensity of 1 sun for 65 h. We consider the revealed BO_2* defect to differ from the BO_2 center, which is responsible for the LID of solar cells, by its local atomic structure where the substitutional boron atom forms direct bonds with two oxygen atoms, as it was assumed in ab initio studies of the structure of BO_2 centers in ref. [12,24,25]. The appearance of new absorption lines and their shift relative to the main transitions for boron is associated with the deformation disturbance experienced by the boron atom from two neighboring oxygen atoms in the atomic structure of the identified BO_2* defect.

This study presents new data on the electronic and vibrational properties of the B_sO_{2i}* defect in boron-doped silicon grown by the Czochralski method. Studies were performed for a set of samples with various levels of boron doping and with oxygen in a wide range of concentrations subjected to heat treatments in the temperature interval of 300–650 °C. The study of boron-related defects in Si subjected to high-temperature treatments are of great importance since such processes are widely used in device manufacturing technologies in both micro and nanoelectronics.

2. Results

2.1. Temperature-Induced Transformation of the Absorption Spectrum of Boron Perturbed by Neighboring O_2

It was shown in ref. [28] that the intensity of the absorption lines at 261.3 and 228 cm^{-1}, corresponding to intracenter transitions for a boron atom perturbed by two neighboring oxygen atoms in the B_sO_{2i}* complex, reach their maximum at 450 °C. Therefore, the Cz-Si:B samples under study were subjected to preliminary heat treatment at 400 °C; afterward, their isochronous annealing was carried out. Due to the weak intensity of the 228 cm^{-1} line, the obtained research results are presented for the more intensive line at 261.3 cm^{-1}.

No new spectral features were found in the absorption spectra of samples subjected to heat treatment in a temperature interval of $T_{ht} \approx 400$–510 °C in addition to those observed earlier. The spectra contained only the lines corresponding to intracenter transitions for boron and the lines, associated with the B_sO_{2i}* defect. Annealing at temperatures exceeding 510 °C results in a decrease in the intensity of 261.3 cm^{-1} line. In a temperature interval of 530–540 °C, the intensity of this line almost did not change; instead, even its slight growth was observed at $T_{ht} \approx 550$ °C. In addition, upon annealing within a temperature interval of 510–540 °C, the position of the line maximum gradually shifted toward higher frequencies up to 261.6 cm^{-1}, and the line became broadened in high-frequency side. In **Figure 1** (1, 2), the fragments of absorption spectra registered after the samples were subjected to heat treatment at 400 and 540 °C are shown.

The shift of the line and its broadening may testify that an additional absorption component appears upon the annealing of the B_sO_{2i}* defect. The line decomposition into components showed that heat treatments at temperatures $T_{ht} > 500$ °C result in the appearance of a new absorption component with a maximum at 261.6 cm^{-1}, which overlaps with the line at 261.3 cm^{-1}. The line decomposition into components is shown in Figure 1 (3, 4).

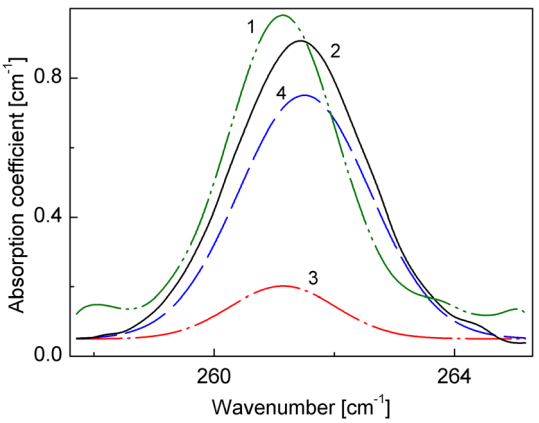

Figure 1. Fragments of the absorption spectra measured at 10 K with the resolution of 0.2 cm^{-1} for Cz-Si:B sample annealed at 400 °C for 10 h (spectrum 1) and subjected to the subsequent heat treatment at 540 °C for 30 min (spectrum 2). Decomposition of the spectrum (2) into components (3, 4) is shown. $N_B = 2.2 \times 10^{16}$ cm^{-3}, $N_O = 1 \times 10^{18}$ cm^{-3}. The spectrum (1) is multiplied by 0.5 for clarity.

It was found that there is a strong correlation between the growth of the intensity of the new absorption component at 261.6 cm^{-1} as the temperature increases and the decrease of the intensity of the line at 261.3 cm^{-1}, which is associated with the B_sO_{2i}* defect. In **Figure 2**, the dependences of the intensities of the 261.3 and 261.6 cm^{-1} lines on the annealing temperature are shown. At heat treatment temperatures exceeding 530 °C, the intensity of the lines was determined by resolving the spectrum into its components. As shown in Figure 2, the 261.3 cm^{-1} line disappears from the spectrum at the annealing temperature $T_{ht} \approx 550$ °C, whereas the component at about 261.6 cm^{-1} reaches its maximum intensity. Within a temperature range of 550–580 °C, we did not observe any noticeable changes in the intensity of the new absorption component. The further growth of the annealing temperature results in the line intensity reduction, and it disappears at a temperature of about 640 °C.

To elucidate the local atomic structure of the defect associated with the registered 261.6 cm^{-1} absorption line, the dependence of the efficiency of its formation on the boron and oxygen concentrations was investigated. To study the dependence on the oxygen content, we used the set of Cz-Si:B samples with boron content of $N_B = 2.2 \times 10^{16}$ cm^{-3} and oxygen concentration varying in the range of $N_O = (4.6–11) \times 10^{17}$ cm^{-3}. **Figure 3**(1) demonstrates the results obtained for samples subjected to heat treatment at $T_{ht} = 540$ °C. As one can see, a

nonlinear dependence of the 261.6 cm^{-1} line intensity on the oxygen concentration is observed. The functional fitting of experimental points, which is also shown in the Figure 3, testifies to a quadratic dependence of the band intensity on the oxygen content in the samples.

To determine the dependence of the formation efficiency of the revealed defect on the boron content, samples with the boron concentration changing in the interval $(0.73–2.2) \times 10^{16}$ cm^{-3} were used. The oxygen concentration was varied in the range of $N_O = (5–10.9) \times 10^{17}$ cm^{-3}. Since the samples under study had different oxygen contents, to avoid errors associated with differences in oxygen concentration and taking into account the quadratic dependence of the 261.6 cm^{-1} line intensity on the oxygen concentration, which is experimentally confirmed in Figure 3(1), the oxygen-normalized intensity of the line was used

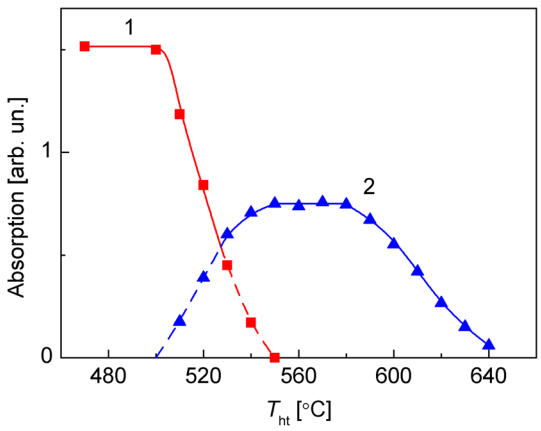

Figure 2. Changes in the intensity of the 261.3 cm^{-1} (1) and 261.6 cm^{-1} (2) absorption lines with the heat treatment temperature.

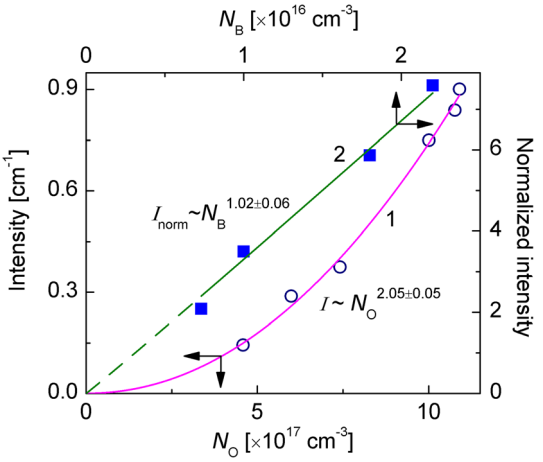

Figure 3. Intensity of the 261.6 cm^{-1} absorption line as a function of oxygen (1) and boron (2) content in the samples Cz-Si:B. $T_{ht} = 540$ °C for 30 min. The points correspond to the experimental data. The solid line is fitted to the measured data.

($I_{norm.}/N_O^2$) to analyze the functional dependence on the boron concentration. Figure 3(2) shows the obtained results. As can be seen, the experimental points are described well by a linear dependence of the efficiency of the registered defect formation on the boron concentration.

Besides the oxygen, carbon impurity in high concentrations [$N_C = (4.9–11.6) \times 10^{16}$ cm^{-3}] was also available in the Cz-Si:B samples under study. Carbon is known to be very active in the defect formation processes, and, under thermal or radiation treatments, it effectively interacts with both boron and oxygen atoms to form a large variety of defects (C_iO_i, C_iB_s, B_iC_s, C_sO_i, and others).[29–35] The study of Cz-Si:B samples with comparable oxygen and boron contents, but with different carbon concentrations, showed that, as for the 261.3 cm^{-1} line, the formation efficiency of the defect responsible for the 261.6 cm^{-1} line is independent of the carbon concentration in the samples.

2.2. Local Vibrational Modes of the BO_2* Defect

When studying the influence of the annealing temperature on intracenter transition for the boron atoms, a change in the intensity of the vibrational mode with a maximum at 1027.5 cm^{-1} was registered. According to previous investigation,[36] the appearance of the vibrational mode is observed in boron-doped silicon and depends on the presence of oxygen in the samples. In **Figure 4**, the absorption spectra registered at room temperature for the as-grown boron-doped Cz-Si samples with various boron and oxygen concentrations, as well as the oxygen-lean Fz-Si:B sample, are shown. One can see that as the boron concentration in the Cz-Si:B samples increases, there appears an additional, rather weak local vibrational mode (LVM) with a maximum at about 1027.5 cm^{-1}. The observed LVM overlaps in the spectrum with the LVM about 1012.7 cm^{-1} associated with dimers. For the oxygen-lean Fz-Si:B sample, no appearance of the 1027.5 cm^{-1} absorption component is observed.

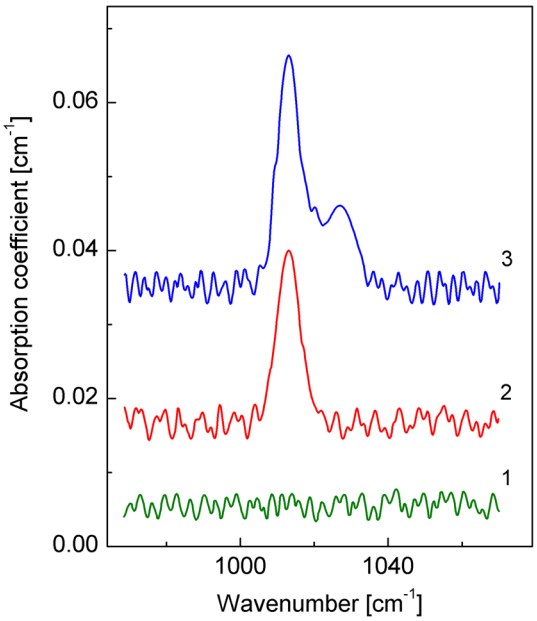

Figure 4. Fragments of the absorption spectra recorded at 300 K for as-grown boron-doped Cz-Si. N_O, $\times 10^{17}$ cm^{-3}: 1-oxygen-lean; 2-9.39; 3-10.9. N_B, $\times 10^{16}$ cm^{-3}: 1-2.6; 2-0.054; 3-2.2. The spectra are base-line corrected and shifted along the vertical axes for clarity.

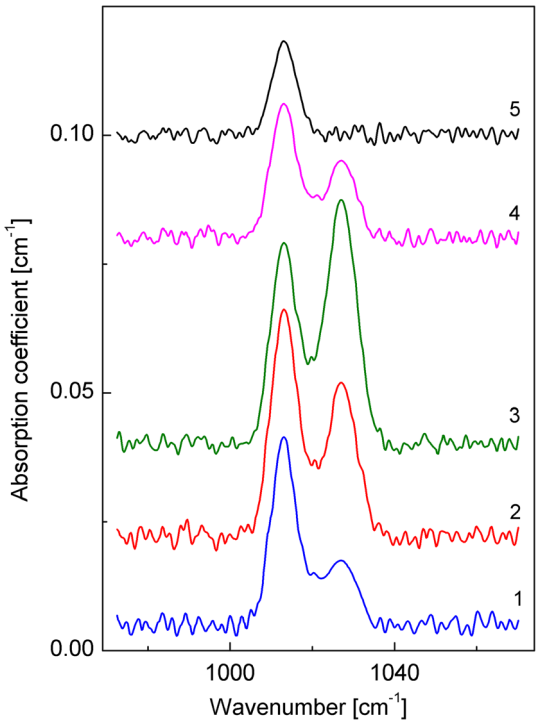

Figure 5. Evolution of the absorption spectrum upon the 1 h isochronal annealing for the boron-doped Cz-Si. The spectra were registered at room temperature. $N_B = 2.2 \times 10^{16}$ cm^{-3}. $N_O = 1.12 \times 10^{18}$ cm^{-3}. T_{ht}, °C: 1- as-grown; 2-380; 3-450; 4-600; 5-650.

It was found that the intensity of the LVM at 1027.5 cm^{-1} and, accordingly, the concentration of the defects responsible for its appearance can vary substantially after the heat treatment of the as-grown samples at elevated temperatures. **Figure 5** demonstrates temperature-induced changes in the intensity of the 1027.5 cm^{-1} vibrational mode for the sample with the oxygen concentration $N_O = 1.12 \times 10^{18}$ cm^{-3} and the boron content $N_B = 2.2 \times 10^{16}$ cm^{-3}. As can be seen from the figure, the intensity of the 1027.5 cm^{-1} LVM rises with increasing heat treatment temperature and reaches its maximum value at $T_{ht} \approx 450$ °C.

An important issue that needs to be solved to understand the nature of the defect responsible for the 1027.5 cm^{-1} vibrational mode is the determination of its local atomic structure. To elucidate the local atomic structure of the defect, we studied the functional dependence of the efficiency of its formation on boron, oxygen, and carbon concentrations. To establish the dependence of the defect formation efficiency on the oxygen content, Cz-Si:B samples with an oxygen concentration varying in the range of (4.6–10.9) $\times 10^{17}$ cm^{-3} and a comparable boron concentration ($N_B = 2.2 \times 10^{16}$ cm^{-3}) were used. **Figure 6**(1) demonstrates the results obtained for samples subjected to heat treatment at 450 °C. As one can see, a nonlinear dependence of the 1027.5 cm^{-1} vibrational mode intensity on the oxygen concentration is observed. The functional fitting of experimental points testifies to a quadratic dependence of the band intensity on the oxygen content in the samples.

To determine the impact of the boron content on the formation of the defect associated with the 1027.5 cm^{-1} mode, we studied Cz-Si samples with the boron concentration of $N_B = (0.73–2.2) \times 10^{16}$ cm^{-3} and the oxygen content varying within the interval $N_O = (5–10.9) \times 10^{17}$ cm^{-3}. Figure 6(2) shows the

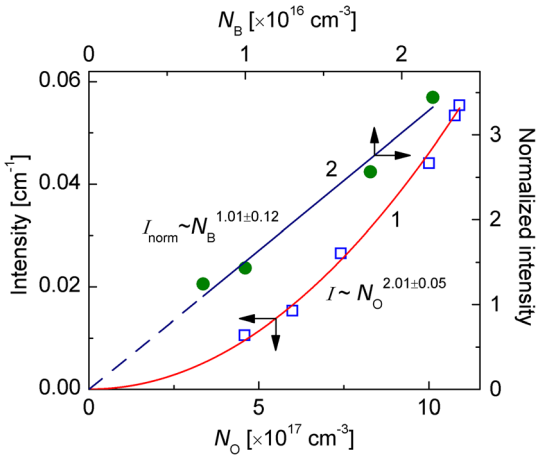

Figure 6. Intensity of the 1027.5 cm^{-1} absorption line as a function of oxygen (1) and boron (2) content in the samples Cz-Si:B. $T_{ht} = 450$ °C for 3 h. The points correspond to the experimental data. The solid line is fitted to the measured data.

obtained dependence of the oxygen-normalized intensity of the 1027.5 cm^{-1} vibrational mode on the substitutional boron concentration for Cz-Si:B samples. As can be seen from Figure 6(2), the experimental points are described well by a linear dependence of the vibrational mode intensity on the boron concentration.

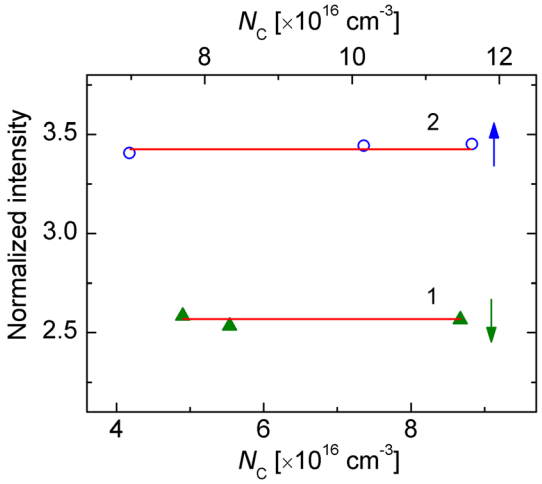

Figure 7. Oxygen-normalized intensity of the 1027 cm^{-1} LVM as a function of carbon content in the samples Cz-Si:B. N_B, × 10^{16} cm^{-3}: 1-1.8; 2-2.2. T_{ht} = 530 °C for 3 h.

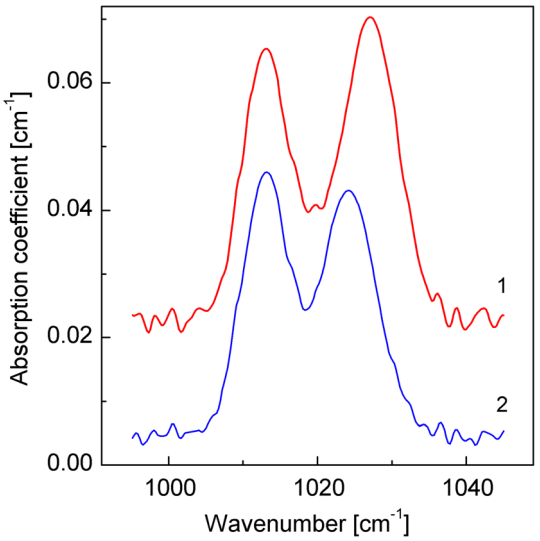

Figure 8. Fragments of the absorption spectra measured at room temperature for boron-doped Cz-Si samples annealed at 500 °C (1) and 530 °C (2). Time of heat treatment T_{ht} = 60 min. $N_B = 2.2 \times 10^{16}$ cm^{-3}, $N_O = 1.12 \times 10^{18}$ cm^{-3}.

To elucidate the possible impact of carbon on the formation of the defect under study, two sets of Cz-Si:B samples with boron contents of 1.8 and 2.2×10^{16} cm^{-3} were used. The carbon concentration was varied within the interval $N_C = (4.9–8.7) \times 10^{16}$ cm^{-3} for the samples with a boron content of $N_B = 1.8 \times 10^{16}$ cm^{-3} and $N_C = (6.9–11.6) \times 10^{16}$ cm^{-3} for the samples with $N_B = 2.2 \times 10^{16}$ cm^{-3}. The oxygen concentration in those samples varied insignificantly, $N_O = (1.0–1.17) \times 10^{18}$ cm^{-3}. The obtained dependence of the oxygen-normalized intensity of the 1027 cm^{-1} band on the carbon concentration is shown in **Figure 7**. It can be seen from the figure that the efficiency of defect formation does not depend on the carbon content in the samples.

It was found that as the annealing temperature T_{ht} exceeds 510 °C, a decrease in the intensity of the vibrational mode at 1027.5 cm^{-1} is observed, and the shift of its maximum toward low frequencies becomes noticeable. At $T_{ht} \approx 540$ °C, the mode maximum shifts to 1024 cm^{-1}. In **Figure 8**, the fragments of absorption spectra registered at annealing temperatures of 500 °C (1) and 530 °C (2) are demonstrated. At higher treatment temperatures, the intensity of this band increases and reaches its maximum value at $T_{ht} \approx 550$ °C.

No changes in the intensity and the position of maximum of the 1024 cm^{-1} LVM occurred in the temperature range of T_{ht} = 550–580 °C. Annealing at temperatures exceeding 580 °C results in a gradual decrease in the LVM intensity, and the band disappears at about 650 °C. Only the 1012 cm^{-1} LVM associated with oxygen dimers is observed in the spectrum (see Figure 5).

The studies showed that the formation efficiency of the defect associated with the 1024 cm^{-1} absorption band, as well as of the complex responsible for the vibrational mode at 1027.5 cm^{-1}, depends quadratically on the oxygen content and linearly on the boron concentration in the samples. Isothermal annealing of the samples showed that the annealing kinetics of the defect responsible for the 1024 cm^{-1} absorption band can be described well by a monoexponential decay, with the activation energy for the defect annealing being equal to ≈3.1 eV.

3. Discussion

The above results indicate that for the boron-oxygen defect responsible for the detected 261.6 cm^{-1} electronic absorption line, a linear dependence of its formation on the boron concentration and a quadratic increase with the oxygen content are observed. This implies that the defect, as well as the registered earlier B_sO_{2i}* complex (electronic transition at 261.3 cm^{-1}), can be identified as B_sO_{2i}. Such a coincidence in the identification of both lines can be related to the following. As was mentioned in the Introduction, according to the consideration of B_sO_{2i} complexes in silicon in the framework of the electron density functional theory, the defect can exist in two stable atomic configurations. The existence of two configurations is assumed both if direct bonds are formed between the boron and two oxygen atoms and if the oxygen atoms are the second neighbors in relation to boron atom.[6,24–26] A strong correlation between the disappearance of the line at 261.3 cm^{-1} and the emergence of a new absorption component about 261.6 cm^{-1} in the course of isochronous annealing, as well as the identical component composition of the defects responsible for the appearance of those two lines in the spectrum, may evidence that annealing results in a temperature-induced transformation in the structural configuration of the B_sO_{2i}* defect. As previously was shown,[28] the activation energy for B_sO_{2i}* annealing is 2.59 ± 0.05 eV. This implies that with this activation energy, the configurational transformation of the B_sO_{2i}* defect occurs.

It should be noted that the shift of the electronic transition from 261.3 to 261.6 cm^{-1} with the change in the atomic configuration is obviously associated with a difference in the deformation perturbation experienced by the boron atoms from the two neighboring oxygen atoms.

The quadratic dependence of the intensity of the 1027.5 cm^{-1} vibrational mode with oxygen content in the samples and the

linear dependence with a boron concentration testify that the defect responsible for the appearance of the vibrational mode can be identified as B_sO_{2i} complex. An analysis of the available literature data on the properties of B_sO_{2i} defects in Czochralski grown boron-doped Si and their comparison with the results obtained in this work testifies that the revealed vibrational mode at 1027.5 cm^{-1} cannot be related to the B_sO_{2i} defect associated with LID of solar cells. The annealing temperature of the B_sO_{2i} center responsible for the solar cells degradation is about 200 °C,[3,6] whereas the defect associated with the 1027.5 cm^{-1} LVM has not yet been formed at this temperature.

A comparative analysis of the temperature-induced changes in the intensities of the vibrational mode at 1027.5 cm^{-1} and the intracenter electronic transition for boron at 261.3 cm^{-1} indicates their strong correlation. The appearance of both lines occurs synchronously and they reach their maximum intensity simultaneously at a temperature of $T_{ht} \approx 450$ °C, when, as is known, oxygen atoms and oxygen dimers diffuse through the Si lattice. Annealing at higher temperatures ($T_{ht} > 510$ °C) results in a decrease in the intensity of both lines and their shift. Besides, as the above results show, the defects responsible for both lines are identified as B_sO_{2i} complexes. Such a correlation in the temperature-induced changes of the intensity of the 261.3 and 1027.5 cm^{-1} lines may suggest that both the electronic transition and the vibrational mode are related to the same center.

The same supposition can be made regarding the electronic transition at 261.6 cm^{-1} and the vibrational mode at 1024 cm^{-1}. As shown above, both lines are related to defects that include a boron atom and an oxygen dimer. A complete coincidence of the temperature changes in their intensities is observed. The lines emerge in the spectrum, rich their maximum intensity and disappear simultaneously at $T_{ht} > 510$, $T_{ht} \approx 550$ and $T_{ht} \approx 650$ °C, respectively. The synchronous changes in the intensities of the 261.6 and 1024 cm^{-1} lines with the treatment temperature may indicate that both lines are related to the same defect.

Thus, the results of the study testify that in both configurations, the B_sO_{2i}* defect that exists in a wide-temperature interval impacts the optical and electronic properties of the material and, accordingly, can affect the parameters of Si:B-based devices.

4. Experimental Section

The samples of boron-doped Si used in the study were grown by the Czochralski (Cz-Si:B) and float-zone (Fz-Si:B) methods. The concentration of boron (N_B) in the samples was varied in the interval $(0.73–2.2) \times 10^{16}$ cm^{-3}. Oxygen (O) and carbon (C) concentrations in samples were determined at room temperature from intensities of the absorption bands associated with vibrational mode of interstitial oxygen (1107 cm^{-1}) and substitutional C atoms (605 cm^{-1}) with the use of calibration coefficients 3.14×10^{17} and 0.94×10^{17} cm^{-2}, correspondingly.[3] The oxygen concentration in the investigated samples was varied from 4.6×10^{17} cm^{-3} to 1.1×10^{18} cm^{-3}, and the carbon concentration was changed in the interval from 4.9×10^{16} cm^{-3} to 1.2×10^{17} cm^{-3}. For comparison, several samples of Fz-Si:B with boron concentration in the range of $(1–2.6) \times 10^{16}$ cm^{-3} were studied.

To study the dependence of the defect formation efficiency in Cz-Si:B on the heat treatment (ht) temperatures and on the main technological impurities of the Cz-Si:B samples, isochronal annealing of the samples was performed in the interval of 400–650 °C. Some samples were subjected to isothermal heat treatments to determine the activation energy for defects annealing. The thermal treatments were carried out in the dark in argon ambient.

The absorption spectra of the samples were studied with the use of a Bruker IFS – 113v Fourier-transform infrared spectrometer. The spectra were recorded at room and 10 K temperatures with a resolution of 0.2–1 cm^{-1}. To determine the absorption associated with the defect under study, the absorption spectrum of high-purity Fz-Si samples with a boron concentration close to the studied was subtracted from spectra.

Conflict of Interest

The authors declare no conflict of interest.

Data Availability Statement

The data that support the findings of this study are available from the corresponding author upon reasonable request.

Keywords

boron, dimers, oxygen, silicon

Received: June 6, 2024
Revised: July 26, 2024
Published online: August 12, 2024

[1] P. Pichler, *Intrinsic Point Defects, Impurities, and their Diffusion in Silicon*, Springer-Verlag, Vienna, Austria **2004**.
[2] S. K. Estreicher, in *Into the Nano Era: Moore's Law Beyond Planar Silicon CMOS*, (Ed: H. R. Huff), Springer, Berlin, Germany **2009**, p. 4.
[3] B. Pajot, B. Clerjaudin, *Optical Absorption of Impurities and Defects in Semiconducting Crystals: Electronic Absorption of Deep Centres and Vibrational Spectra* (Eds: M. Cardona, P. Fulde, K. von Klitzing, R. Merlin, H.-J. Queisser, H. Störmer), Springer-Verlag, Berlin, Germany **2013**.
[4] B. Lim, F. Rougieux, D. Macdonald, K. Bothe, J. Schmidt, *J. Appl. Phys.* **2010**, *108*, 103722.
[5] J. Schmidt, B. Lim, D. Walter, K. Bothe, S. Gatz, T. Dullweber, P. P. Altermatt, *IEEE J. Photovolt.* **2013**, *3*, 114.
[6] T. Niewelt, J. Schön, W. Warta, S. W. Glunz, M. C. Schubert, *IEEE J. Photovolt.* **2017**, *7*, 383.
[7] B. Hallam, A. Herguth, P. Hamer, N. Nampalli, S. Wilking, M. Abbott, S. Wenham, G. Hahn, *Appl. Sci.* **2018**, *8*, 10.
[8] J. Schmidt, A. G. Aberle, R. Hezel, in *Proc. of the 26th IEEE Photovoltaic Specialists Conf., Anaheim, California, USA*, IEEE, New York **1997**, p. 13.
[9] J. Schmidt, A. Cuevas, *J. Appl. Phys.* **1999**, *86*, 3175.
[10] J. Bourgoin, N. de Angelis, G. Strobl, in *Proc. of the 16th European Photovoltaic Solar Energy Conf., Glasgow, UK*, James & James, London **2000**, p. 1356.
[11] K. Bothe, R. Hezel, J. Schmidt, *Appl. Phys. Lett.* **2003**, *83*, 1125.
[12] J. Schmidt, K. Bothe, *Phys. Rev. B* **2004**, *69*, 024107.
[13] A. Herguth, G. Schubert, M. Kaes, G. Hahn, in *Proc. of the 21st European Photovoltaic Solar Energy Conf., Dresden, Germany*, WIP Renewable Energies, Munich **2006**, p. 530.
[14] M. Sanati, S. K. Estreicher, *Phys. Rev. B* **2005**, *72*, 165206.
[15] K. Bothe, J. Schmidt, *J. Appl. Phys.* **2006**, *99*, 01370.

[16] B. Lim, K. Bothe, J. Schmidt, *Phys. Status Solidi Rapid Res. Lett.* **2008**, *2*, 93.
[17] A. Herguth, G. Hahn, *J. Appl. Phys.* **2010**, *108*, 114509.
[18] D. Shen, C. Sun, P. Zheng, D. Macdonald, F. Rougieux, *Jpn. J. Appl. Phys.* **2017**, *56*, 08MB23.
[19] Y. Wu, X. Yu, P. Chen, X. Chen, D. Yang, *Appl. Phys. Lett.* **2014**, *104*, 102108.
[20] V. Voronkov, R. Falster, *Phys. Status Solidi C* **2016**, *13*, 712.
[21] J. Geilker, W. Kwapil, S. Rein, *J. Appl. Phys.* **2011**, *109*, 053718.
[22] M. Kim, M. Abbott, N. Nampalli, S. Wenham, B. Stefani, B. Hallam, *J. Appl. Phys.* **2017**, *121*, 053106.
[23] M. Vaqueiro-Contreras, V. P. Markevich, J. Coutinho, P. Santos, I. F. Crowe, M. P. Halsall, I. Hawkins, S. B. Lastovskii, L. I. Murin, A. R. Peaker, *J. Appl. Phys.* **2019**, *125*, 185704.
[24] J. Adey, R. Jones, D. W. Palmer, P. R. Briddon, S. Öberg, *Phys. Rev. Lett.* **2004**, *93*, 055504.
[25] J. Schmidt, K. Bothe, D. Macdonald, J. Adey, R. Jones, D. W. Palmer, *J. Mater. Res.* **2006**, *21*, 5.
[26] M.-H. Du, H. M. Branz, R. S. Crandall, S. B. Zhang, *Phys. Rev. Lett.* **2006**, *97*, 256602.
[27] L. Khirunenko, M. Sosnin, A. Duvanskii, N. Abrosimov, H. Riemann, *Phys. Status Solidi A* **2021**, *218*, 2100181.
[28] L. Khirunenko, M. Sosnin, A. Duvanskii, N. Abrosimov, H. Riemann, *J. Appl. Phys.* **2022**, *132*, 135703.
[29] R. D. Harris, J. L. Newton, G. D. Watkins, *Phys. Rev. B* **1987**, *36*, 1094.
[30] P. J. Drevinsky, C. E. Caefer, S. P. Tobin, J. C. Mikkelsen Jr., L. C. Kimerling, in *MRS Symposia Proc. Vol. 104: Defects in Electronic Materials* (Eds: M. Stavola, S. J. Pearton, G. Davies, Materials Research Society, Pittsburgh, PA **1988**, p. 167.
[31] L. C. Kimerling, M. T. Asom, J. L. Benton, P. J. Drevinsky, C. E. Caefer, *Mater. Sci. Forum* **1989**, *38*, 141.
[32] J. Adey, R. Jones, P. R. Briddon, J. P. Goss, *J. Phys.: Condens. Matter* **2003**, *15*, S2851.
[33] J. Adey, J. P. Goss, R. Jones, P. R. Briddon, *Phys. Rev. B* **2003**, *67*, 245325.
[34] N. Yarykin, O. V. Feklisova, J. Weber, *Phys. Rev. B* **2004**, *69*, 045201.
[35] L. I. Khirunenko, M. G. Sosnin, A. V. Duvanskii, N. V. Abrosimov, H. Riemann, *Phys. Rev. B* **2016**, *94*, 235210.
[36] L. I. Khirunenko, Yu. V. Pomozov, M. G. Sosnin, *Semiconductors* **2013**, *47*, 269.